Angular Scattering Properties of Metasurfaces

Karim Achouri and Olivier J. F. Martin

***Abstract*— This article aims at studying the angular scattering properties of bianisotropic metasurfaces and clarifying the different roles played by tangential and normal polarization densities. Different types of metasurfaces are considered for this study and are classified according to their symmetrical/asymmetrical and reciprocal/nonreciprocal angular scattering behavior. Finally, the article presents the relationships between the symmetrical angular scattering properties of reciprocal metasurfaces and the structural symmetries of their scattering particles. This may prove to be practically useful for the implementation of metasurfaces with complex angular scattering characteristics.**

***Index Terms*— Bianisotropy, generalized sheet transition conditions (GSTCs), metasurface, normal polarizations, reciprocity, susceptibility tensor, symmetry.**

I. Introduction

METASURFACES are electrically thin surfaces engineered to control the propagation of electromagnetic waves. In the past few years, they have attracted major attention due to their unprecedented and unmatched capabilities in manipulating light [1]–[5]. They are typically composed of a periodic array of sub-wavelength scattering particles designed to provide a specified scattering response.

In order to model, simulate and implement these structures, several metasurface synthesis and analysis techniques have been developed based on different approaches. For instance, metasurfaces have been modeled based on impedance/admittance matrices [6], [7], susceptibility tensors [5], [8], [9] and polarizability tensors [10], [11]. These techniques have generally in common the concept of modeling metasurfaces as zero-thickness sheets exhibiting effective material parameters. In addition, they also usually ignore the presence of normal polarizations (or currents) with respect to the metasurface plane, although some works have tackled this topic such as [9], [12]–[14]. The rationale being that normal polarizations may be ignored since electromagnetic fields can be expressed solely in terms of their tangential field components according to the Huygens principle [15, pp. 376–385]. The legitimate question of whether normal polarizations are useful in bringing new functionalities to metasurfaces, or could they be simply ignored and replaced by purely tangential polarizations, was then raised [16], [17]. As will be succinctly explained thereafter, normal polarizations may indeed be ignored *if* a metasurface is always excited with the same illumination conditions, e.g., same incidence angle. However, if the incidence angle is changed, then the presence of normal polarizations do play a role in the scattering behavior of metasurfaces and should not be ignored. Additionally, normal polarizations may even be leveraged to bring about new functionalities as demonstrated in [18].

This article aims at studying the angular scattering behavior of bianisotropic metasurfaces with both tangential and normal polarization densities and clarify the role played by the latter. In particular, we will see how different susceptibility components affect the angular scattering of metasurfaces. For this purpose, we will restrict our attention to *uniform* metasurfaces, i.e., metasurfaces exhibiting effective material parameters that are *not* spatially varying. This is a necessary restriction that is required to properly assess the effect of the presence of these susceptibility components. We will also discuss how the metasurface scattering particles structural symmetries may be related to the presence of certain susceptibility components [19]. This aspect cannot provide the exact geometry and dimensions of the scattering particles but can at least provide valuable information about the structural symmetries that they should exhibit, which may be of practical interest for designing metasurfaces with complex angular scattering properties.

This article is organized as follows. Section II provides general information regarding the application of the Huygens principle and the various different types of symmetrical/asymmetrical and reciprocal/nonreciprocal scattering properties of metasurfaces. Section III presents the angular scattering properties of different types of metasurfaces. Section IV discusses the relationships between the angular scattering symmetries and the scattering particles structural symmetries. Finally, Section V concludes this article.

II. General Considerations

Before delving into the angular scattering properties of metasurfaces and discussing how they may be affected by the structural symmetries of the their scattering particles, we shall first understand how normal polarization densities affect their electromagnetic response and how they can be used to bring about new functionalities.

Let us consider the generalized sheet transition conditions (GSTCs), which accurately relate the electromagnetic fields interacting with a metasurface to its material parameters [7], [20, pp. 67–69], [21]. Throughout this article, we will consider that a metasurface may be modeled as a zero-thickness sheet of polarizable elements lying in the xy plane at

Manuscript received January 14, 2019; revised August 5, 2019; accepted August 5, 2019. Date of publication September 30, 2019; date of current version January 3, 2020. This work was supported by the European Research Council under Grant ERC-2015-AdG-695206 Nanofactory. *(Corresponding author: Karim Achouri.)*

The authors are with the Nanophotonics and Metrology Laboratory, Department of Microengineering, École Polytechnique Fédérale de Lausanne, 1015 Lausanne, Switzerland (e-mail: karim.achouri@epfl.ch).

Color versions of one or more of the figures in this article are available online at http://ieeexplore.ieee.org.

Digital Object Identifier 10.1109/TAP.2019.2943423

0018-926X © 2019 IEEE. Personal use is permitted, but republication/redistribution requires IEEE permission.
See http://www.ieee.org/publications_standards/publications/rights/index.html for more information.

Authorized licensed use limited to: EPFL LAUSANNE. Downloaded on July 07,2020 at 09:05:10 UTC from IEEE Xplore. Restrictions apply.

$z = 0$, we will also consider the time-dependence $e^{j\omega t}$, which we will omit for conciseness. It follows that the GSTCs read:

$$\hat{z} \times \Delta\mathbf{H} = j\omega\mathbf{P} - \hat{z} \times \nabla M_z \tag{1a}$$

$$\hat{z} \times \Delta\mathbf{E} = -j\omega\mu_0\mathbf{M} - \frac{1}{\epsilon_0}\hat{z} \times \nabla P_z \tag{1b}$$

where $\Delta\mathbf{E} = \mathbf{E}^+ - \mathbf{E}^-$ and $\Delta\mathbf{H} = \mathbf{H}^+ - \mathbf{H}^-$ are the difference of the electric and magnetic fields on both sides of the metasurface with the superscripts $+$ and $-$ referring to the fields at $z = 0^+$ and $z = 0^-$, respectively, and $\mathbf{P}$ and $\mathbf{M}$ are the electric and magnetic surface polarization densities induced on the metasurface. In the case of a bianisotropic metasurface, these polarization densities may be expressed in terms of the average electric and magnetic fields on both sides of the metasurfaces as [21]

$$\mathbf{P} = \epsilon_0\overline{\overline{\chi}}_{\text{ee}} \cdot \mathbf{E}_{\text{av}} + \epsilon_0\eta_0\overline{\overline{\chi}}_{\text{em}} \cdot \mathbf{H}_{\text{av}} \tag{2a}$$

$$\mathbf{M} = \overline{\overline{\chi}}_{\text{mm}} \cdot \mathbf{H}_{\text{av}} + \frac{1}{\eta_0}\overline{\overline{\chi}}_{\text{me}} \cdot \mathbf{E}_{\text{av}} \tag{2b}$$

where ϵ_0 is the vacuum permittivity associated with the vacuum impedance, η_0, and $\overline{\overline{\chi}}_{\text{ee}}$, $\overline{\overline{\chi}}_{\text{mm}}$, $\overline{\overline{\chi}}_{\text{em}}$ and $\overline{\overline{\chi}}_{\text{me}}$ are the electric, magnetic, electro-magnetic and magneto-electric susceptibility tensors, respectively.

In the most general case, the GSTCs in (1) are differential equations due to the presence of the spatial derivatives of P_z and M_z. Moreover, each of the susceptibility tensors in (2) includes both normal and tangential susceptibility components, which amounts to a total of 36 susceptibilities. This makes the modeling of metasurfaces a particularly difficult task. This is one the reasons why it has been common practice to ignore the presence of normal susceptibility components and accordingly discard the spatial derivatives in the GSTCs [9].

These simplifications are notably justified by three main considerations.

1) In many cases, metasurfaces have been realized for paraxial wave propagation (close to normal incidence) for which the normal components of the electric and magnetic fields are negligible compared to their tangential parts. Therefore, the scattering contributions emerging from the normal polarizations are also negligible.
2) Metasurfaces are very thin compared to the operation wavelength meaning that, irrespectively of the wave propagating angle, the response of the surface is more important in its tangential directions than in its normal direction.
3) The Huygens principle stipulates that an electromagnetic field can always be expressed in terms of its tangential components. Therefore, a metasurface with both normal and tangential susceptibility components can be transformed into an equivalent metasurface with only tangential susceptibility components such that both metasurfaces exhibit the same scattering response [16], [17], as depicted in Fig. 1(a) and (b).

This last point can be easily verified from the GSTCs. Indeed, from (1a), we see that $\mathbf{P}$ is on an equal footing with the gradient of M_z and similarly $\mathbf{M}$ is on an equal footing with the gradient of P_z in (1b). This means that M_z (P_z) can be transformed into an effective and purely tangential electric (magnetic) polarization, $\mathbf{P}_{\text{eff}}$ ($\mathbf{M}_{\text{eff}}$).

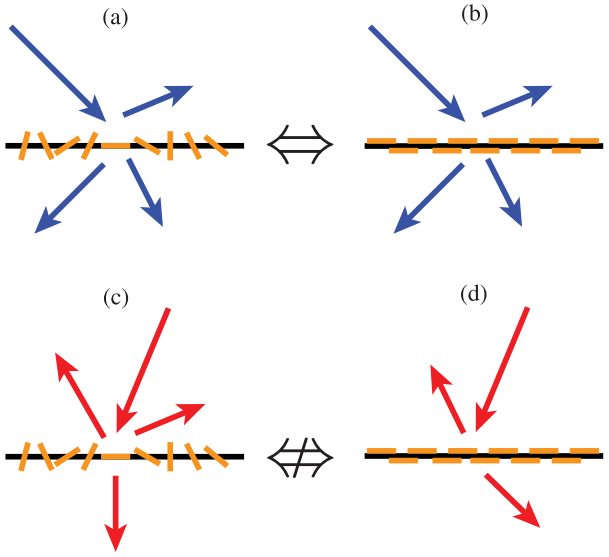

Fig. 1. Illustrations of the application of the Huygens principle and its limitation. (a) Metasurface with complex orientations of scattering particles in both vertical and horizontal directions. (b) Metasurface equivalent to (a) but with purely tangential scattering particles, which produces the same scattering as the metasurface in (a). (c) Metasurface in (a) is now excited at another incidence angle and produces different scattered fields than in (a). (d) Purely tangential metasurface (b) is not the equivalent of the one in (c) anymore.

While these three points are generally valid, they also carry their own limitations.

1) Metasurfaces can be designed for waves with large propagation angles, making the normal components of their fields actually larger than their corresponding tangential field components.
2) Simple conductive rings or loops within the metasurface plane are sufficient to generate strong normal magnetic responses even in the case of paraxial wave propagation.
3) The application of the Huygens principle to the implementation of metasurfaces with purely tangential polarizations and which exhibit the same scattering response as metasurfaces possessing both normal and tangential polarizations, as depicted in Fig. 1(a) and (b), is of course correct.

However, its validity is generally restricted to the case of identical excitations. Indeed, this stems from the presence of the gradients of the polarizations in (1), which typically limits the validity of the effective purely tangential polarizations, $\mathbf{P}_{\text{eff}}$ and $\mathbf{M}_{\text{eff}}$, to the case of fixed illumination. It is followed that if the illumination angle is changed, then the purely tangential metasurface will, in general, not produce the same scattering as the original metasurface. This is depicted in Fig. 1(c) and (d), where the metasurface in Fig. 1(c) is structurally identical to that in Fig. 1(a) but scatters differently than the metasurface in Fig. 1(d), which is yet structurally identical to that in Fig. 1(b).

From these considerations, it follows that the usefulness of the normal polarizations depends upon how a metasurface is used in practice. If it is meant to be illuminated always

Authorized licensed use limited to: EPFL LAUSANNE. Downloaded on July 07,2020 at 09:05:10 UTC from IEEE Xplore. Restrictions apply.

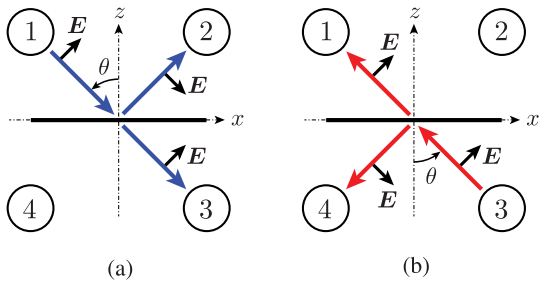

Fig. 2. Incidence angle and field polarization for (a) downward wave incidence and (b) upward wave incidence.

at the same incidence angle, then the presence of normal polarizations may be ignored. However, if a metasurface is meant to be illuminated at many different incidence angles, then the normal polarizations cannot be ignored and they may even be utilized to bring about additional functionalities, as will be shown thereafter.

One of the main functionalities that the presence of normal polarizations may add to the already impressive arsenal of field manipulation capabilities of metasurfaces, is their ability in controlling the angular scattering response of the latter, which has been only little studied [18], [22]. In order to understand how the angular scattering response of a metasurface depends upon its susceptibilities, we shall next consider a simplified but yet relevant and pedagogical scenario.

Let us consider a *uniform* metasurface surrounded by vacuum on both sides and illuminated with a plane wave impinging at an incidence angle θ. This plane wave is reflected and transmitted by the metasurface without rotation of polarization and at the same angle θ due to the uniformity of the structure. We consider the case where the scattering occurs only in the xz plane and the waves are all p-polarized. The case of s-polarized waves is very similar and is thus not discussed here for briefness. The four quadrants of the xz plane are each associated with a "port," which may serve either as a source or a receiver. The metasurface may then be excited from any of these ports, as illustrated in Fig. 2. It follows that port 1 can only communicate to port 2 via reflection and to port 3 via transmission and can never exchange energy with port 4. And so on for the other ports.

With this approach, we can now easily characterize the angular scattering response of any metasurface. It turns out that there are two main properties that apply in transmission and/or in reflection and which are the properties of *reciprocity* and *symmetry*.[1] In order to understand and visualize what these properties correspond to, one should refer to Fig. 3 in which we have depicted the four different possible types of reciprocal/nonreciprocal scattering and the eight different possible types of symmetric/asymmetric scattering. We have labeled each of these twelve different cases to be able to easily identify them thereafter.

[1]Here "symmetry" refers to the symmetry of the angular scattering behavior of a metasurface. In Sections III and IV, we will relate the angular scattering properties of symmetry to the structural symmetries of the scattering particles composing the metasurface.

In the top row of Fig. 3, we present the different transmission cases and have thus not drawn the reflected waves for conciseness. Similarly, the bottom row of the figure only represents the different reflection cases for which we have not drawn the transmitted waves.

For the four reciprocal cases, the metasurface is either reciprocal, if the blue and red arrows represent the same quantity (e.g., $T_{31} = T_{13}$ and/or $R_{12} = R_{21}$,...) or nonreciprocal if they are not the same (e.g., $T_{31} \neq T_{13}$ or $R_{12} \neq R_{21}$,...). Similarly, a metasurface would exhibit the property of forward horizontal transmission symmetry (FHTS) if $T_{31} = T_{24}$, and so on.

From Fig. 3, one may *a priori* think that a metasurface has the capability to independently control any of these twelve cases. However, such a feature is not physically possible as some of these properties are actually connected to each other. Indeed, a reciprocal metasurface (one that simultaneously exhibits all four reciprocal properties) has all of its transmission/reflection properties which depend on each other, i.e., FHTS $\equiv$ BHTS $\equiv$ DVTS $\equiv$ UVTS and FHRS $\equiv$ BHRS $\equiv$ FCRS $\equiv$ BCRS. This means that a reciprocal metasurface, which, for instance, satisfies FHTS will also automatically satisfy BHTS, DVTS and UVTS. Thus, a reciprocal metasurface is either: 1) symmetric in both transmission and reflection; 2) asymmetric in both reflection and transmission; 3) symmetric only in transmission; or 4) symmetric only in reflection.

Similar relationships exist if only some of the four reciprocity conditions are satisfied. For instance, if only the condition of forward transmission reciprocity (FTR) is fulfilled, i.e., $T_{13} = T_{31}$, $T_{24} \neq T_{42}$, $R_{12} \neq R_{21}$ and $R_{34} \neq T_{43}$, then the metasurface can be completely asymmetric in reflection. However, the following transmission symmetry properties would be equivalent to each other: FHTS $\equiv$ UVTS and BHTS $\equiv$ DVTS, thus limiting the capabilities of the metasurface in controlling transmitted waves. This is one example that shows how the concept of nonreciprocity is not just limited to the implementation of isolators but may also be leveraged for additional field manipulations capabilities [9].

It follows that the symmetric/asymmetric scattering properties of metasurfaces are directly related to their reciprocal/nonreciprocal characteristics. This means that the more nonreciprocal a metasurface is, the more degrees of freedom it generally has to control its angular scattering. As said above, there are four types of metasurfaces with different angular scattering properties that could be realized when the four reciprocal cases of Fig. 3 are satisfied. When three reciprocal cases are satisfied, then there are 32 different types of metasurfaces that are realizable. If two reciprocal cases are satisfied, then 96 different types of metasurfaces can be realized. Finally, if only one or none of the reciprocal cases are satisfied, then a total of 256 could be realized.

In order to easily identify the scattering properties of a metasurface, we have introduced the diagrammatic representation depicted in Fig. 4, which corresponds to a metasurface with scattering properties arbitrarily chosen for illustration. This type of diagram represents the four ports surrounding the metasurface (note placed in the same configuration as in Figs. 2 and 3 for better visualization) and the corresponding

Authorized licensed use limited to: EPFL LAUSANNE. Downloaded on July 07,2020 at 09:05:10 UTC from IEEE Xplore. Restrictions apply.

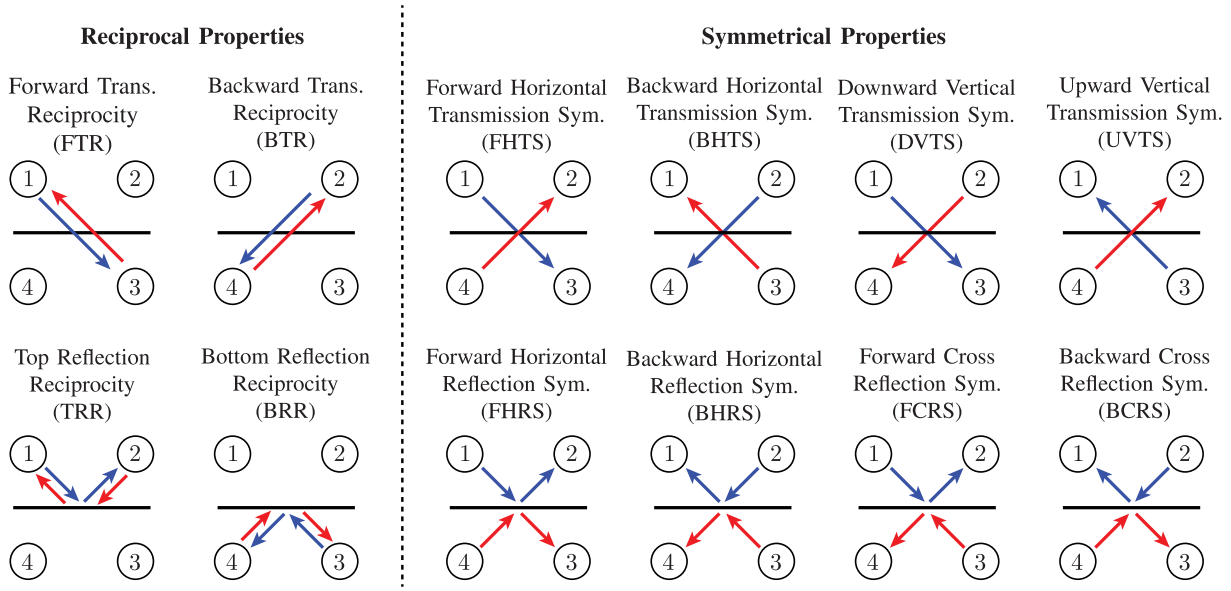

Fig. 3. Representations of the 12 different possible sorts of scattering.

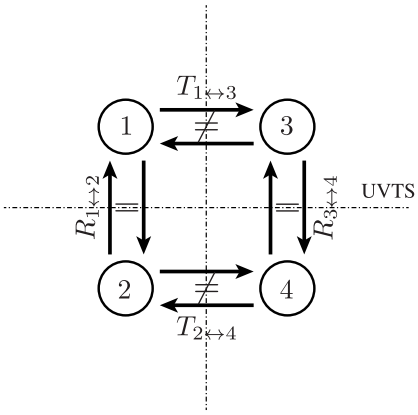

Fig. 4. Pictorial representation of the scattering properties of a metasurface. The signs $=$ and $\neq$, respectively, indicate a reciprocal or a nonreciprocal transmission/reflection relation between two ports. The vertical dashed line indicates that the metasurface exhibits all symmetric reflection properties. The horizontal dashed line with the label UVTS indicates that this metasurface only exhibits this particular transmission symmetry property.

transmission and reflection relations between them. A reciprocal relation is indicated with an "=" sign, while a nonreciprocal relation is indicated with a "≠" sign. The vertical dashed line without any label signifies that this metasurface exhibits all reflection symmetries. The horizontal dashed line with the label UVTS indicates that only this transmission symmetry is satisfied. This diagram thus allows one to identify at a glance what are the angular scattering properties of any metasurface.

III. Angular Scattering Properties of Uniform Metasurfaces

In this section, we present the angular transmission and reflection coefficients for four different types of uniform metasurfaces. Specifically, we present the case of birefringent metasurfaces with only tangential polarizations, anisotropic metasurfaces with both tangential and normal polarizations, bianisotropic metasurfaces with only tangential polarizations and bianisotropic metasurfaces with tangential and normal polarizations. For each of these cases, we provide numerical simulations of reciprocal metasurfaces with actual scattering particles.

In order to properly assess the angular scattering behavior of these metasurfaces in terms of their susceptibilities, we derive the expressions of their scattering parameters.[2] To do so, we first have to define the difference and average of the fields in (1) and (2). Using the convention adopted in Fig. 2, we have at $z = 0$ that

$$\Delta\mathbf{E} = \pm\hat{x}\frac{k_z}{k_0}(1 + R - T) \tag{3a}$$

$$\Delta\mathbf{H} = \hat{y}\frac{1}{\eta_0}(-1 + R + T) \tag{3b}$$

$$E_{x,\mathrm{av}} = \frac{k_z}{2k_0}(1 + T + R) \tag{3c}$$

$$E_{z,\mathrm{av}} = \frac{k_x}{2k_0}(1 + T - R) \tag{3d}$$

$$H_{y,\mathrm{av}} = \mp\frac{1}{2\eta_0}(1 + T - R) \tag{3e}$$

where $k_z = k_0\cos\theta$ and $k_x = k_0\sin\theta$ and where we have dropped the term $e^{-jk_x x}$ for conciseness. Top (bottom) signs correspond to incident waves propagating backward (forward) along z, as in Fig. 2(a) [see Fig. 2(b)].

Now, one can obtain the transmission and reflection coefficients of any metasurface simply by substituting (3) into (1) and (2) and solving the resulting system of equations for the parameters T and R, respectively. The material properties of the metasurface are encoded into its susceptibilities and one can thus decide what type of metasurface to study just by setting to zero the susceptibility components that are

[2]Note that the values of retrieved susceptibilities may depend upon the angle of wave propagation due to coupling effects between scattering particles and spatial dispersion. For practical purposes, we do not take into account these effects as they do not affect the general goal of this work, which is to study the relationships between susceptibilities, scattering behavior and symmetries.

Authorized licensed use limited to: EPFL LAUSANNE. Downloaded on July 07,2020 at 09:05:10 UTC from IEEE Xplore. Restrictions apply.

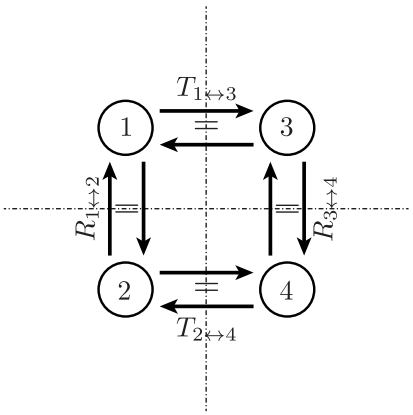

Fig. 5. Angular scattering properties of a birefringent metasurface.

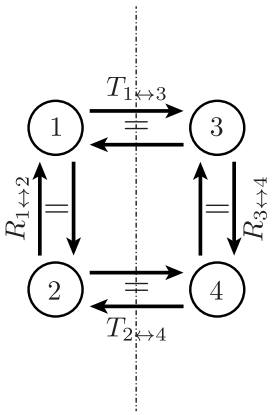

Fig. 6. Angular scattering properties of a reciprocal anisotropic metasurface.

not desired. Note that if a metasurface is reciprocal, then some of its susceptibility components are related to each other as stipulated by the Lorentz reciprocity theorem [15]. Accordingly, the susceptibility tensors of a reciprocal metasurface must satisfy the following reciprocity conditions:

$$\overline{\overline{\chi}}_{\mathrm{ee}}^{\mathrm{T}} = \overline{\overline{\chi}}_{\mathrm{ee}}, \qquad \overline{\overline{\chi}}_{\mathrm{mm}}^{\mathrm{T}} = \overline{\overline{\chi}}_{\mathrm{mm}}, \qquad \overline{\overline{\chi}}_{\mathrm{me}}^{\mathrm{T}} = -\overline{\overline{\chi}}_{\mathrm{em}}. \tag{4}$$

A contrario, a nonreciprocal metasurface does not satisfy at least one of these conditions.

A. Birefringent Metasurfaces

We now start by considering the case of birefringent metasurfaces, which is the most conventional and simple type of metasurface. Assuming p-polarized waves, the only susceptibility components that are excited on such a metasurface are χ_{ee}^{xx} and χ_{mm}^{yy}. This metasurface thus does not exhibit any normal polarization and is always fully reciprocal according to (4). The corresponding angular scattering parameters are given by

$$R = \frac{2j\left(k_0^2\chi_{\mathrm{mm}}^{yy} - k_z^2\chi_{\mathrm{ee}}^{xx}\right)}{\left(2 + jk_z\chi_{\mathrm{ee}}^{xx}\right)\left(2k_z + jk_0^2\chi_{\mathrm{mm}}^{yy}\right)} \tag{5a}$$

$$T = \frac{k_z\left(4 + k_0^2\chi_{\mathrm{mm}}^{yy}\chi_{\mathrm{ee}}^{xx}\right)}{\left(2 + jk_z\chi_{\mathrm{ee}}^{xx}\right)\left(2k_z + jk_0^2\chi_{\mathrm{mm}}^{yy}\right)}. \tag{5b}$$

We can directly see that these coefficients do not depend on k_x meaning that changing the incidence angle from θ to $-\theta$ will not change the response of the metasurface. Moreover, illuminating the metasurface from the top or from the bottom does not affect its response either. We conclude that such a metasurface is fully symmetrical in addition of being fully reciprocal. Its corresponding diagrammatic representation is thus that of Fig. 5.

We now present a realization of such a birefringent metasurface. Let us consider the unit cell structure of Fig. 8(a), which composes the metasurface with a square lattice period of 200 nm. The unit cell is composed of two identical gold rods separated by 50 nm. They have a square cross section of 40×40 nm and a length of 170 nm. This unit cell structure is thus perfectly symmetric in the x-, y- and z-directions, which results in the expected fully symmetrical behavior. The resulting transmission (solid lines) and reflection (dashed lines) amplitude and phase, computed using a full-wave commercial software, are plotted in Fig. 8(e) and (i), respectively.

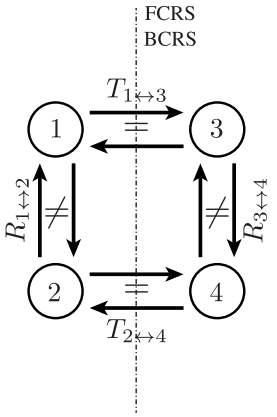

Fig. 7. Angular scattering properties of a nonreciprocal anisotropic metasurface.

B. Anisotropic Metasurfaces

We now discuss the more general case of anisotropic metasurfaces. For the considered case of p-polarization, the only susceptibilities excited on such metasurfaces are χ_{ee}^{xx}, χ_{ee}^{xz}, χ_{ee}^{zx}, χ_{ee}^{zz} and χ_{mm}^{yy}. The resulting scattering parameters are given by

$$R = \frac{2}{C_{\mathrm{a}}}\left[k_0^2\chi_{\mathrm{mm}}^{yy} - k_z^2\chi_{\mathrm{ee}}^{xx} + k_xk_z\left(\chi_{\mathrm{ee}}^{zx} - \chi_{\mathrm{ee}}^{xz}\right) + k_x^2\chi_{\mathrm{ee}}^{zz}\right] \tag{6a}$$

$$T = \frac{jk_z}{C_{\mathrm{a}}}\left[2jk_x\left(\chi_{\mathrm{ee}}^{xz} + \chi_{\mathrm{ee}}^{zx}\right) + k_x^2\left(\chi_{\mathrm{ee}}^{xz}\chi_{\mathrm{ee}}^{zx} - \chi_{\mathrm{ee}}^{xx}\chi_{\mathrm{ee}}^{zz}\right) - 4 - k_0^2\chi_{\mathrm{ee}}^{xx}\chi_{\mathrm{mm}}^{yy}\right] \tag{6b}$$

$$C_{\mathrm{a}} = 2\left(k_z^2\chi_{\mathrm{ee}}^{xx} + k_x^2\chi_{\mathrm{ee}}^{z} + k_0^2\chi_{\mathrm{mm}}^{yy}\right) + jk_z\left[k_x^2\left(\chi_{\mathrm{ee}}^{xx}\chi_{\mathrm{ee}}^{zz} - \chi_{\mathrm{ee}}^{xz}\chi_{\mathrm{ee}}^{zx}\right) - 4 + k_0^2\chi_{\mathrm{ee}}^{xx}\chi_{\mathrm{mm}}^{yy}\right] \tag{6c}$$

where T and R are the same whether the metasurface is illuminated from the top or from the bottom. This already provides an important information that this type of metasurfaces always satisfies *at least* the conditions of FCRS and BCRS. In addition, we also see the presence of k_x for both the transmission and the reflection coefficients. We can thus

Authorized licensed use limited to: EPFL LAUSANNE. Downloaded on July 07,2020 at 09:05:10 UTC from IEEE Xplore. Restrictions apply.

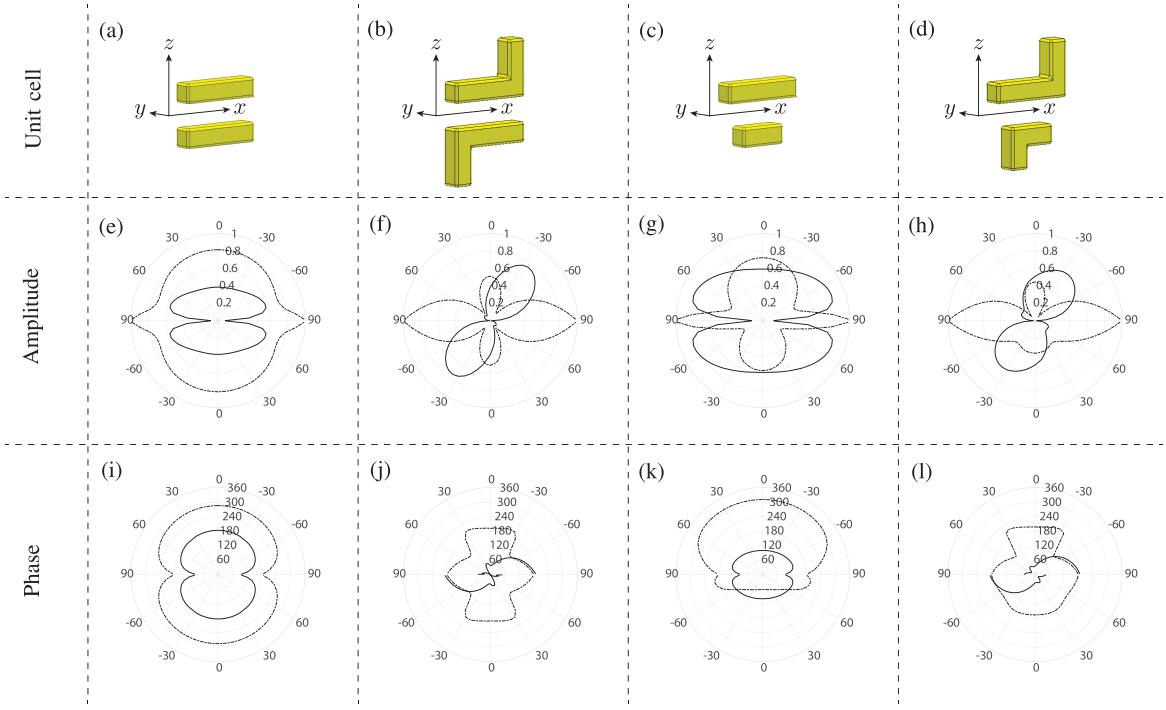

Fig. 8. Angular scattering properties of four different reciprocal metasurfaces. Top row: metasurface unit cells which are periodically arranged in the xy plane with a square lattice period of 200 nm to form the corresponding metasurfaces. Middle row: amplitude of the transmission (solid lines) and reflection (dashed–dotted lines) coefficients versus incidence angle. Note that the angular coordinate of these plots corresponds to the incidence angle θ following the convention adopted in Fig. 2(a) and (b). Bottom row: phase of the transmission and reflection coefficients. The unit cells in (a) and (c) have been simulated at $\lambda_0 = 600$ nm, while the unit cells (b) and (d) have been simulated at $\lambda_0 = 660$ nm.

infer that this type of metasurfaces may present some form of asymmetric scattering in both transmission and reflection. To be more specific, we next consider the cases of reciprocal and nonreciprocal scattering separately.

Let us first consider the case of a reciprocal metasurface for which $\chi_{\mathrm{ee}}^{xz} = \chi_{\mathrm{ee}}^{zx}$ according to (4). In this case, we see that k_x disappears in (6a), leaving only k_x^2 in its numerator and denominator. This confirms the reciprocal behavior of this metasurface as the reflection coefficient remains the same for incidence angles θ and $-\theta$. In contrast, the coefficient k_x does not disappear in (6b) meaning that such a metasurface is transmission asymmetric. As a result, this type of metasurface may be represented by the diagrammatic illustration of Fig. 6.

In order to verify the angular scattering properties of such a metasurface, we have designed the unit cell shown in Fig. 8(b). It has the same dimensions as the structure in Fig. 8(a) with the addition of two vertical rods with a length of 75 nm. As can be seen in the simulation results of Fig. 8(f) and (j), the metasurface is perfectly symmetric in reflection and exhibits a strong angular asymmetric transmission.

Let us now consider the case where the metasurface is nonreciprocal, i.e., when $\chi_{\mathrm{ee}}^{xz} \neq \chi_{\mathrm{ee}}^{zx}$. Then again, the metasurface is completely transmission asymmetric. Except in the very particular scenario where $\chi_{\mathrm{ee}}^{xz} = -\chi_{\mathrm{ee}}^{zx}$, in which case the term k_x vanishes in the nominator of (6b) and the metasurface becomes fully symmetric in transmission. Besides that particular case, such a metasurface is only nonreciprocal in reflection, while being fully reciprocal in transmission. Indeed, the term k_x does not vanish in (6a) leading to a nonreciprocal reflection coefficient and since the scattering parameters are the same irrespectively of the illumination side, the metasurface is always reciprocal in transmission. In addition, such a metasurface always satisfies the properties of FCRS and BCRS since the reflection coefficient is the same for both sides but different for θ and $-\theta$. It follows that, for the general case of nonreciprocal scattering (i.e., when $\chi_{\mathrm{ee}}^{xz} \neq \pm\chi_{\mathrm{ee}}^{zx}$), the diagrammatic representation of this metasurface is that of Fig. 7.

It is important to consider that the asymmetry of this anisotropic metasurface, whether it is reciprocal or not, is directly related to the presence of the term k_x and not that of k_x^2 since the latter is a symmetric function of θ. Upon inspection of (6), we see that the presence of k_x is related to the presence of χ_{ee}^{xz} and χ_{ee}^{zx}, while χ_{ee}^{zz} is essentially related to k_x^2. It follows that the susceptibility components χ_{ee}^{xz} and χ_{ee}^{zx} are responsible for the asymmetric angular scattering of this metasurface. In fact, it would be difficult to distinguish between a metasurface where the only nonzero normal susceptibility is χ_{ee}^{zz} and the birefringent metasurfaces of Section III-A since χ_{ee}^{zz} does not break the scattering symmetry of the structure. The only way to know whether the metasurface exhibits a nonzero χ_{ee}^{zz} component would be to compute its scattering parameters for at least two different incidence angles and then solving (6) to obtain χ_{ee}^{zz}.

C. Bianisotropic Metasurfaces With Only Tangential Polarizations

Let us now consider the case of bianisotropic metasurfaces with only tangential polarizations densities for which,

Authorized licensed use limited to: EPFL LAUSANNE. Downloaded on July 07,2020 at 09:05:10 UTC from IEEE Xplore. Restrictions apply.

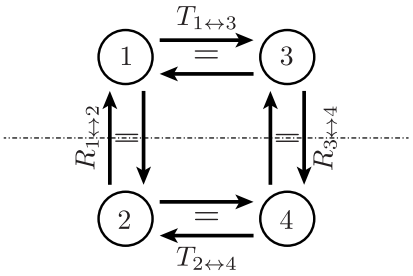

Fig. 9. Angular scattering properties of a reciprocal bianisotropic metasurface with only tangential polarizations.

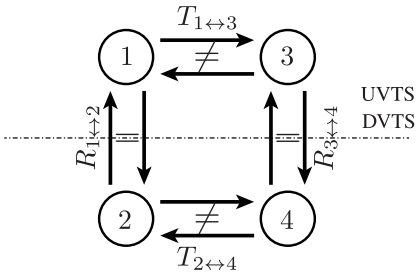

Fig. 10. Angular scattering properties of a nonreciprocal bianisotropic metasurface with only tangential polarizations.

assuming p-polarization, only the following susceptibilities are excited: χ_{ee}^{xx}, χ_{mm}^{yy}, χ_{em}^{xy} and χ_{me}^{yx}. The corresponding scattering parameters are given by

$$R = \frac{2k_0^2\chi_{\mathrm{mm}}^{yy} - 2k_z\left[k_z\chi_{\mathrm{ee}}^{xx} \mp k_0\left(\chi_{\mathrm{me}}^{yx} - \chi_{\mathrm{em}}^{xy}\right)\right]}{k_z\left[2k_z\chi_{\mathrm{ee}}^{xx} - j\left(4 + k_0^2\chi_{\mathrm{em}}^{xy}\chi_{\mathrm{me}}^{yx}\right)\right] + k_0^2\left(2 + jk_z\chi_{\mathrm{ee}}^{xx}\right)\chi_{\mathrm{mm}}^{yy}} \tag{7a}$$

$$T = \frac{jk_z\left[\left(2j \mp k_0\chi_{\mathrm{em}}^{xy}\right)\left(2j \mp k_0\chi_{\mathrm{me}}^{yx}\right) - k_0^2\chi_{\mathrm{ee}}^{xx}\chi_{\mathrm{mm}}^{yy}\right]}{k_z\left[2k_z\chi_{\mathrm{ee}}^{xx} - j\left(4 + k_0^2\chi_{\mathrm{em}}^{xy}\chi_{\mathrm{me}}^{yx}\right)\right] + k_0^2\left(2 + jk_z\chi_{\mathrm{ee}}^{xx}\right)\chi_{\mathrm{mm}}^{yy}} \tag{7b}$$

where the top signs correspond to incident waves propagating backward along z, as in Fig. 2(a), while the bottom signs correspond to incident waves propagating forward as in Fig. 2(b).

As can be seen, these expressions do not depend on k_x. We can thus directly infer that the scattering response is the same for incidence angles of θ and $-\theta$. Moreover, the fact that the scattering parameters are not the same for top and bottom illuminations indicates that such a metasurface must exhibit some form of asymmetric scattering. In order to be more specific, we again separate the cases of reciprocal and nonreciprocal scattering.

Let us first discuss the case when the metasurface is reciprocal, i.e., when $\chi_{\mathrm{em}}^{xy} = -\chi_{\mathrm{me}}^{yx}$ according to (4). When this reciprocity condition is satisfied, the transmission coefficient in (7b) becomes the same for top and bottom illuminations. It follows that the transmission coefficient is fully reciprocal and symmetric. However, the dependence on the illumination side does not vanish for the reflection coefficient in (7a), meaning that such a metasurface is completely reflection asymmetric. The corresponding diagrammatic representation is depicted in Fig. 9.

From these considerations, we must conclude that the bianisotropic susceptibilities χ_{em}^{xy} and χ_{me}^{yx} are nonzero when a metasurface presents a structural asymmetry in its normal direction. Concretely, the metasurface does not "look" the same when seen from both sides. Such a peculiar property may, for instance, allow one to control the reflection phase or the matching condition depending on the illumination side. This has been notably leveraged in [23] to implement fully efficient refractive metasurfaces, where the incident and refracted beams can both be matched even though they propagate at different angles.

In order to demonstrate the angular scattering properties of this type of metasurfaces, we have designed the unit cell of Fig. 8(c). It consists of two rods with a respective length of 170 and 100 nm. The two rods do not have the same length such that the metasurface is structurally asymmetric with respect to its normal direction. The resulting amplitude and phase of the scattering parameters are respectively plotted in Fig. 8(g) and (k), where we indeed retrieve the expected asymmetric reflection behavior.

Now, let us consider the case where the metasurface is nonreciprocal, i.e., when $\chi_{\mathrm{em}}^{xy} \neq -\chi_{\mathrm{me}}^{yx}$. We know that the dependence on the illumination side does not vanish anymore and the metasurface is thus nonreciprocal in transmission. However, the metasurface remains reciprocal in reflection because of the absence of k_x term in (7). Due to the structural asymmetry and the nonreciprocal transmission properties of such a metasurface, only the transmission symmetries UVTS and DVTS are satisfied. It follows that the diagrammatic representation of such a metasurface is that of Fig. 10.

Note that there is a special case of nonreciprocity where $\chi_{\mathrm{em}}^{xy} = \chi_{\mathrm{me}}^{yx}$. If this equality is satisfied, then the reflection coefficient becomes the same for top and bottom illuminations and the metasurface thus becomes fully reflection symmetric.

Finally, we would like to discuss a very peculiar but particularly interesting case of bianisotropic metasurfaces, which is when $\chi_{\mathrm{ee}}^{xx} = \chi_{\mathrm{mm}}^{yy} = 0$ and $\chi_{\mathrm{em}}^{xy} \neq 0$ and $\chi_{\mathrm{me}}^{yx} \neq 0$. In such a scenario, the scattering parameters in (7) reduce to

$$R = \pm\frac{2jk_0\left(\chi_{\mathrm{em}}^{xy} - \chi_{\mathrm{me}}^{yx}\right)}{4 + k_0^2\chi_{\mathrm{em}}^{xy}\chi_{\mathrm{me}}^{yx}} \tag{8a}$$

$$T = \frac{\left(2 \pm jk_0\chi_{\mathrm{em}}^{xy}\right)\left(2 \pm jk_0\chi_{\mathrm{me}}^{yx}\right)}{4 + k_0^2\chi_{\mathrm{em}}^{xy}\chi_{\mathrm{me}}^{yx}}. \tag{8b}$$

The particular characteristics of such a metasurface is that it does not exhibit any angular dependence, i.e., the coefficients (8) do not contain k_x or k_z. Accordingly, its scattering is the same irrespectively of the incidence angle. One example of such a metasurface is when $\chi_{\mathrm{em}}^{xy} = -\chi_{\mathrm{me}}^{yx} = -2j/k_0$. In this case, the resulting metasurface is reciprocal, passive and lossless (according to the corresponding hermitian conditions [15]) and behaves as a perfect magnetic conductor ($R = 1$ and $T = 0$) when illuminated from the top and a perfect electric conductor ($R = -1$ and $T = 0$) when illuminated from bottom.

D. Bianisotropic Metasurfaces With Tangential and Normal Polarizations

We shall now consider the most general type of metasurfaces under p-polarized excitation, which is that of

Authorized licensed use limited to: EPFL LAUSANNE. Downloaded on July 07,2020 at 09:05:10 UTC from IEEE Xplore. Restrictions apply.

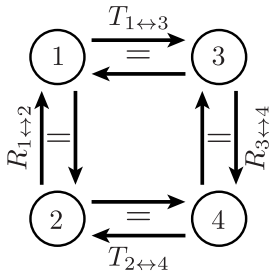

Fig. 11. Angular scattering properties of a reciprocal bianisotropic metasurface with tangential and normal polarizations.

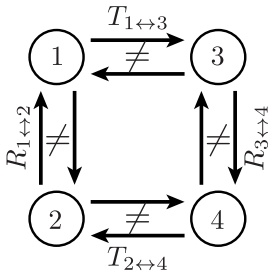

Fig. 12. Angular scattering properties of a nonreciprocal bianisotropic metasurface with tangential and normal polarizations.

bianisotropic metasurfaces with both tangential and normal polarizations. The susceptibility components that may be excited on such metasurfaces are: $\chi_{\rm ee}^{xx}$, $\chi_{\rm ee}^{xz}$, $\chi_{\rm ee}^{zx}$, $\chi_{\rm ee}^{zz}$, $\chi_{\rm mm}^{yy}$, $\chi_{\rm em}^{xy}$, $\chi_{\rm me}^{yx}$, $\chi_{\rm em}^{zy}$ and $\chi_{\rm me}^{yz}$. The corresponding scattering parameters are given as

$$R = \frac{2}{C_{\rm b}}\{k_x^2\chi_{\rm ee}^{zz} - k_z^2\chi_{\rm ee}^{xx} - k_z[k_x(\chi_{\rm ee}^{xz} - \chi_{\rm ee}^{zx}) \mp k(\chi_{\rm em}^{xy} - \chi_{\rm me}^{yx})] \mp kk_x(\chi_{\rm em}^{zy} + \chi_{\rm me}^{yz}) + k^2\chi_{\rm mm}^{yy}\} \quad (9a)$$

$$T = \frac{jk_z}{C_{\rm b}}\{k_x^2(\chi_{\rm ee}^{xz}\chi_{\rm ee}^{zx} - \chi_{\rm ee}^{xx}\chi_{\rm ee}^{zz}) + (2j \mp k\chi_{\rm em}^{xy})(2j \mp k\chi_{\rm me}^{yx}) + k_x[\chi_{\rm ee}^{zx}(2j \mp k\chi_{\rm em}^{xy}) + \chi_{\rm ee}^{xz}(2j \mp k\chi_{\rm me}^{yx}) \pm k\chi_{\rm ee}^{xx}(\chi_{\rm em}^{zy} + \chi_{\rm me}^{yz})] - k^2\chi_{\rm ee}^{xx}\chi_{\rm mm}^{yy}\}. \quad (9b)$$

$$C_{\rm b} = 2[k_z^2\chi_{\rm ee}^{xx} + k_x^2\chi_{\rm ee}^{zz} \mp kk_x(\chi_{\rm em}^{zy} + \chi_{\rm me}^{yz}) + k^2\chi_{\rm mm}^{yy}] \pm k^2(\chi_{\rm ee}^{xx}\chi_{\rm mm}^{yy} - \chi_{\rm em}^{xy}\chi_{\rm me}^{yx}) - jk_z[k_x^2(\chi_{\rm ee}^{xz}\chi_{\rm ee}^{zx} - \chi_{\rm ee}^{xx}\chi_{\rm ee}^{zz}) + 4 \mp kk_x \times(\chi_{\rm ee}^{zx}\chi_{\rm em}^{xy} + \chi_{\rm ee}^{xz}\chi_{\rm me}^{yx} - \chi_{\rm ee}^{xx}(\chi_{\rm em}^{z} + \chi_{\rm me}^{yz}))] \quad (9c)$$

where, as before, the top signs correspond to illumination from the top and the bottom signs to illumination from the bottom. As may be expected, combining the effects of $\chi_{\rm ee}^{xz}$ and $\chi_{\rm ee}^{zx}$, and $\chi_{\rm em}^{xy}$ and $\chi_{\rm me}^{yx}$, leads to metasurfaces that have the capabilities of being completely asymmetric in both reflection and transmission. As explained before, the presence of $\chi_{\rm ee}^{zz}$ is "neutral" in the sense that this susceptibility is related to k_x^2, which is a symmetric function of θ. The presence of $\chi_{\rm em}^{zy}$ and $\chi_{\rm me}^{yz}$ plays a role that is similar to that of $\chi_{\rm ee}^{xz}$ and $\chi_{\rm ee}^{zx}$ since both sets of susceptibilities are related to the presence of k_x. However, if the metasurface is reciprocal, then $\chi_{\rm em}^{zy}$ and $\chi_{\rm me}^{yz}$ cancel each other in (9) (since by reciprocity: $\chi_{\rm em}^{zy} = -\chi_{\rm me}^{yz}$) and thus do not play a role in the scattering. These two susceptibilities may thus be used as a mean to break the angular scattering symmetries but only in nonreciprocal metasurfaces.

Let us now consider the case where the metasurface is reciprocal, which according to (4), implies that the following conditions are simultaneously satisfied $\chi_{\rm ee}^{xz} = \chi_{\rm ee}^{zx}$, $\chi_{\rm em}^{xy} = -\chi_{\rm me}^{yx}$ and $\chi_{\rm em}^{zy} = -\chi_{\rm me}^{yz}$. As explained above, this type of metasurface is completely asymmetric and thus corresponds to the diagrammatic representation of Fig. 11. Such asymmetric angular scattering properties may, for instance, be achieved with the unit cell design of Fig. 8(d), where the horizontal rods have a length of 170 nm and 100 nm, and the vertical rods have a length of 75 nm and 45 nm. The resulting amplitude and phase of the scattering parameters are respectively plotted in Fig. 8(h) and (l) where the expected angular asymmetric scattering behavior is indeed retrieved. Note that this unit cell has been essentially designed by mixing together the unit cells of Fig. 8(b) and (c).

TABLE I

SYMMETRY RELATIONSHIPS BETWEEN ANGULAR SCATTERING AND UNIT CELL STRUCTURE FOR THE FOUR TYPES OF RECIPROCAL METASURFACES. C_2 REFERS TO A TWOFOLD (180°) ROTATION SYMMETRY AROUND THE Y-AXIS, WHILE σ_z AND σ_x REFER TO REFLECTION SYMMETRIES THROUGH THE Z-AXIS AND THE X-AXIS, RESPECTIVELY

Type	Reflection	Transmission	Structure
Birefringent $\chi_{\rm ee}^{xx}$, $\chi_{\rm mm}^{yy}$	$C_2\sigma_z$	$C_2\sigma_z$	$C_2\sigma_z$ (or σ_x)
Anisotropic $\chi_{\rm ee}^{xx}$, $\chi_{\rm mm}^{yy}$ $\chi_{\rm ee}^{xz}$, $\chi_{\rm ee}^{zx}$, $\chi_{\rm ee}^{zz}$	$C_2\sigma_z$	C_2	C_2
Bianisotropic $\chi_{\rm ee}^{xx}$, $\chi_{\rm mm}^{yy}$ $\chi_{\rm em}^{xy}$, $\chi_{\rm me}^{yx}$	σ_z	$C_2\sigma_z$	σ_z
Bianisotropic $\chi_{\rm ee}^{xx}$, $\chi_{\rm mm}^{yy}$, $\chi_{\rm ee}^{zz}$ $\chi_{\rm ee}^{xz}$, $\chi_{\rm ee}^{zx}$, $\chi_{\rm em}^{xy}$, $\chi_{\rm me}^{yx}$, $\chi_{\rm em}^{zy}$, $\chi_{\rm me}^{yz}$	σ_z	C_2	–

In the case where the metasurface is nonreciprocal and that all conditions provided above are not satisfied, then both reflection and transmission coefficients are nonreciprocal in addition of being asymmetric. This leads to the diagrammatic representation of Fig. 12.

Due to the complexity of this type of metasurfaces, there are several different "special cases" of nonreciprocity that may also occur. We do not discuss them here since they would be particularly difficult to implement in practice. Nevertheless, we have considered some of these special cases and have included their corresponding angular scattering properties in Table II.

Note that in Table II, the susceptibilities associated with the four types of metasurfaces are only indicative. Indeed, as said above, it is impossible to make the difference between a birefringent metasurface whose only nonzero susceptibilities are $\chi_{\rm ee}^{xx}$ and $\chi_{\rm mm}^{yy}$ and a metasurface whose nonzero susceptibilities are $\chi_{\rm ee}^{xx}$, $\chi_{\rm mm}^{yy}$ and $\chi_{\rm ee}^{zz}$ since $\chi_{\rm ee}^{zz}$ is not related to an asymmetric function of θ.

IV. RELATIONS BETWEEN SCATTERING SYMMETRIES AND STRUCTURAL SYMMETRIES

A close inspection of the scattering particles in Fig. 8 suggests the possibility to relate their structural symmetries

Authorized licensed use limited to: EPFL LAUSANNE. Downloaded on July 07,2020 at 09:05:10 UTC from IEEE Xplore. Restrictions apply.

TABLE II

PROPERTIES OF SYMMETRY AND RECIPROCITY FOR DIFFERENT TYPES OF METASURFACES CLASSIFIED FOLLOWING THE CONVENTION ADOPTED IN FIG. 3. FOR EACH CATEGORY, THE METASURFACE IS EITHER SYMMETRIC/RECIPROCAL (✓) OR ASYMMETRIC/NONRECIPROCAL (✗). THE LABEL "(SC)" INDICATES A SPECIAL CASE OF NONRECIPROCITY

Type	Reciprocity	FTR	BTR	FHTS	BHTS	DVTS	UVTS	TRR	BRR	FHRS	BHRS	FCRS	BCRS
Birefringent χ_{ee}^{xx}, χ_{mm}^{yy}	✓	✓	✓	✓	✓	✓	✓	✓	✓	✓	✓	✓	✓
Anisotropic χ_{ee}^{xx}, χ_{mm}^{yy} χ_{ee}^{xz}, χ_{ee}^{zx}, χ_{ee}^{zz}	✓ $\chi_{\text{ee}}^{xz} = \chi_{\text{ee}}^{zx}$	✓	✓	✗	✗	✗	✗	✓	✓	✓	✓	✓	✓
	✗ $\chi_{\text{ee}}^{xz} \neq \chi_{\text{ee}}^{zx}$	✓	✓	✗	✗	✗	✗	✗	✗	✗	✗	✓	✓
	✗ (SC) $\chi_{\text{ee}}^{xz} = -\chi_{\text{ee}}^{zx}$	✓	✓	✗	✗	✗	✗	✗	✗	✗	✗	✓	✓
Bianisotropic χ_{ee}^{xx}, χ_{mm}^{yy} χ_{em}^{xy}, χ_{me}^{yx}	✓ $\chi_{\text{em}}^{xy} = -\chi_{\text{me}}^{yx}$	✓	✓	✓	✓	✓	✓	✓	✓	✗	✗	✗	✗
	✗ $\chi_{\text{em}}^{xy} \neq -\chi_{\text{me}}^{yx}$	✗	✗	✗	✗	✓	✓	✓	✓	✗	✗	✗	✗
	✗ (SC) $\chi_{\text{em}}^{xy} = \chi_{\text{me}}^{yx}$	✗	✗	✗	✗	✓	✓	✓	✓	✓	✓	✓	✓
Bianisotropic χ_{ee}^{xx}, χ_{mm}^{yy}, χ_{ee}^{zz} χ_{ee}^{xz},χ_{ee}^{zx}, χ_{em}^{xy}, χ_{me}^{yx},χ_{em}^{zy}, χ_{me}^{yz}	✓ $\chi_{\text{ee}}^{xz} = \chi_{\text{ee}}^{zx}$ $\chi_{\text{em}}^{xy} = -\chi_{\text{me}}^{yx}$ $\chi_{\text{em}}^{zy} = -\chi_{\text{me}}^{yz}$	✓	✓	✗	✗	✗	✗	✓	✓	✗	✗	✗	✗
	✗ $\chi_{\text{ee}}^{xz} \neq \chi_{\text{ee}}^{zx}$ $\chi_{\text{em}}^{xy} \neq -\chi_{\text{me}}^{yx}$ $\chi_{\text{em}}^{zy} \neq -\chi_{\text{me}}^{yz}$	✗	✗	✗	✗	✗	✗	✗	✗	✗	✗	✗	✗
	✗ (SC) $\chi_{\text{ee}}^{xz} = \chi_{\text{ee}}^{zx}$ $\chi_{\text{em}}^{xy} = \chi_{\text{me}}^{yx}$ $\chi_{\text{em}}^{zy} = \pm\chi_{\text{me}}^{yz}$	✗	✗	✗	✗	✗	✗	✗	✗	✓	✓	✗	✗
	✗ (SC) $\chi_{\text{ee}}^{xz} = \pm\chi_{\text{ee}}^{zx}$ $\chi_{\text{em}}^{xy} = \mp\chi_{\text{me}}^{yx}$ $\chi_{\text{em}}^{zy} = \chi_{\text{me}}^{yz}$	✗	✗	✗	✗	✗	✗	✗	✗	✗	✗	✗	✗
	✗ (SC) $\chi_{\text{ee}}^{xz} = -\chi_{\text{ee}}^{zx}$ $\chi_{\text{em}}^{xy} = -\chi_{\text{me}}^{yx}$ $\chi_{\text{em}}^{zy} = \pm\chi_{\text{me}}^{yz}$	✗	✗	✓	✓	✗	✗	✗	✗	✗	✗	✗	✗
	✗ (SC) $\chi_{\text{ee}}^{xz} = -\chi_{\text{ee}}^{zx}$ $\chi_{\text{em}}^{xy} = \chi_{\text{me}}^{yx}$ $\chi_{\text{em}}^{zy} = -\chi_{\text{me}}^{yz}$	✗	✗	✗	✗	✓	✓	✗	✗	✗	✗	✓	✓

to their corresponding angular scattering properties. In what follows, we thus discuss the relationships between the angular scattering symmetries and the structural symmetries of different scattering particles and deduce some general rules that may be useful to design metasurfaces with specific angular scattering properties.

In the forthcoming discussion, we assume that the origin of the coordinate system lies in the center of the scattering particles. We also consider that the scattering particles exhibit a plane reflection symmetry with respect to the xz plane such as those in Fig. 8. The more general case where the scattering particles do not exhibit an xz plane reflection symmetry will be the topic of a future work.

Let us first consider the case where the metasurfaces are reciprocal, which leads to the four different types of scattering behavior presented in Fig. 8. From this figure, we observe that there are three possible types of symmetries [24, pp. 5–10]: a 180°-rotation symmetry around the y-axis (C_2), a reflection symmetry through the x-axis (σ_x) and a reflection symmetry through the z-axis (σ_z). Accordingly, we report, in Table I, the symmetries of the reflection and transmission coefficients as well as those of the corresponding scattering particles for these four types of reciprocal metasurfaces.

The first important deduction is that reciprocity necessarily implies that the reflection coefficients have a σ_z symmetry, while the transmission coefficients have a C_2 symmetry. Note that this statement is valid irrespective of the geometry of the scattering particles. The second deduction is that the angular scattering properties of a given reciprocal metasurface always exhibit the same symmetries as those of its scattering particles.

Accordingly, if the scattering particles do not exhibit any structural symmetry, then the resulting metasurface corresponds to a bianisotropic structure with both normal and tangential polarization densities and its angular scattering response does not present any symmetry besides those imposed by reciprocity (last row in Table I). If the scattering particles are *only* σ_z symmetric, then the metasurface is bianisotropic with only tangential polarizations. If the scattering particles are *only* C_2 symmetric, then the metasurface is anisotropic with both normal and tangential polarizations. Finally, if the scattering particles are both C_2 and σ_z symmetric, then the metasurface is birefringent, i.e., like that shown in Fig. 8(e) and (i).

At this point, it should be emphasized that the three possible symmetries (σ_x, σ_z and C_2) are connected to each other such that if a structure (or an angular scattering diagram as those in Fig. 8) exhibits both C_2 and σ_z symmetries, then it necessarily also exhibits a σ_x symmetry due to the fundamental property that $C_2 \cdot \sigma_z = \sigma_x$ [24, pp. 5–10]. For instance, the scattering particle in Fig. 8(a) is C_2 and σ_z

Authorized licensed use limited to: EPFL LAUSANNE. Downloaded on July 07,2020 at 09:05:10 UTC from IEEE Xplore. Restrictions apply.

symmetric and it is also de facto σ_x symmetric. However, the equality $C_2 \cdot \sigma_z = \sigma_x$ may be confusing in some cases. Indeed, take for instance the scattering particle in Fig. 8(b) and flip the bottom L-shaped structure by 180° around the z-axis such that it corresponds to the mirror reflection of the top L-shaped structure. Such a scattering particle would neither be σ_z symmetric nor C_2 symmetric but it would be σ_x symmetric and would thus exhibit an angular scattering response that is equivalent to that of a birefringent metasurface.

Besides the classification of Tables I and II in terms of metasurface types, we can assert the following relationships between structural symmetries and presence of susceptibilities.

1) A scattering particle with full structural symmetry ($C_2\sigma_z$ or σ_x) corresponds to an effective zero-thickness material which exhibits nonzero χ_{ee}^{xx} and χ_{mm}^{yy} components (and probably also χ_{ee}^{zz} to a lesser extent).
2) A scattering particle with only C_2 symmetry exhibits *at least* nonzero χ_{ee}^{xz} and χ_{ee}^{zx} components.
3) A scattering particle with only σ_z symmetry is related to the presence of *at least* χ_{em}^{xy} and χ_{me}^{yx}.
4) A scattering particle without any structural symmetry must *at least* exhibit the following susceptibility components: χ_{ee}^{xz}, χ_{ee}^{zx}, χ_{em}^{xy} and χ_{me}^{yx}.

So far, we have discussed the symmetries associated with reciprocal metasurfaces. Accordingly, we have presented, in Table I, the four main types of reciprocal metasurfaces and the corresponding four possible combinations of scattering particle symmetries. A nonreciprocal metasurface must somehow be able to break the reciprocal angular scattering symmetries, i.e., σ_z symmetry for the reflection and C_2 symmetry for the transmission. This is obviously impossible to achieve simply by controlling the geometrical properties of the particles but rather requires the introduction of either: a time-odd bias, a time-varying modulation or some form of nonlinear interactions.

V. Conclusion

In this article, we have shed some light on the role played by both tangential and normal polarization densities on the angular scattering properties of bianisotropic metasurfaces. To do so, we have considered different types of uniform metasurfaces and have investigated their angular scattering responses in terms of their susceptibilities. We have shown that the angular scattering properties of a metasurface may generally be classified according to 12 different categories composed of four types of reciprocal/nonreciprocal scattering and eight types of symmetrical/asymmetrical scattering. Finally, we have deduced relationships between the structural symmetries of the metasurface scattering particles and the corresponding symmetries of their angular scattering response. This may prove very useful in designing the metasurface scattering particles that achieve asymmetric angular scattering.

References

[1] N. Yu and F. Capasso, "Flat optics with designer metasurfaces," *Nature Mater.*, vol. 13, pp. 139–150, Jan. 2014.

[2] C. Pfeiffer, N. K. Emani, A. M. Shaltout, A. Boltasseva, V. M. Shalaev, and A. Grbic, "Efficient light bending with isotropic metamaterial Huygens' surfaces," *Nano Lett.*, vol. 14, no. 5, pp. 2491–2497, Apr. 2014.

[3] S. B. Glybovski, S. A. Tretyakov, P. A. Belov, Y. S. Kivshar, and C. R. Simovski, "Metasurfaces: From microwaves to visible," *Phys. Rep.*, vol. 634, pp. 1–72, May 2016.

[4] A. E. Minovich, A. E. Miroshnichenko, A. Y. Bykov, T. V. Murzina, D. N. Neshev, and Y. S. Kivshar, "Functional and nonlinear optical metasurfaces," *Laser Photon. Rev.*, vol. 9, no. 2, pp. 195–213, Mar. 2015.

[5] K. Achouri and C. Caloz, "Design, concepts, and applications of electromagnetic metasurfaces," *Nanophotonics*, vol. 7, no. 6, pp. 1095–1116, Jun. 2018.

[6] C. Pfeiffer and A. Grbic, "Metamaterial Huygens' surfaces: Tailoring wave fronts with reflectionless sheets," *Phys. Rev. Lett.*, vol. 110, May 2013, Art. no. 197401.

[7] M. Selvanayagam and G. V. Eleftheriades, "Circuit modeling of Huygens surfaces," *IEEE Antennas Wireless Propag. Lett.*, vol. 12, pp. 1642–1645, Dec. 2013.

[8] K. Achouri, B. A. Khan, S. Gupta, G. Lavigne, M. A. Salem, and C. Caloz, "Synthesis of electromagnetic metasurfaces: Principles and illustrations," *EPJ Appl. Metamater.*, vol. 2, p. 12, Oct. 2015.

[9] K. Achouri, M. A. Salem, and C. Caloz, "General metasurface synthesis based on susceptibility tensors," *IEEE Trans. Antennas Propag.*, vol. 63, no. 7, pp. 2977–2991, Jul. 2015.

[10] Y. Ra'di, V. S. Asadchy, and S. A. Tretyakov, "Tailoring reflections from thin composite metamirrors," *IEEE Trans. Antennas Propag.*, vol. 62, no. 7, pp. 3749–3760, Jul. 2014.

[11] T. Niemi, A. O. Karilainen, and S. A. Tretyakov, "Synthesis of polarization transformers," *IEEE Trans. Antennas Propag.*, vol. 61, no. 6, pp. 3102–3111, Jun. 2013.

[12] C. L. Holloway, M. A. Mohamed, E. F. Kuester, and A. Dienstfrey, "Reflection and transmission properties of a metafilm: With an application to a controllable surface composed of resonant particles," *IEEE Trans. Antennas Propag.*, vol. 47, no. 4, pp. 853–865, Nov. 2005.

[13] C. Holloway, E. F. Kuester, J. Gordon, J. O'Hara, J. Booth, and D. Smith, "An overview of the theory and applications of metasurfaces: The two-dimensional equivalents of metamaterials," *IEEE Antennas Propag. Mag.*, vol. 54, no. 2, pp. 10–35, Apr. 2012.

[14] M. Albooyeh, S. Tretyakov, and C. Simovski, "Electromagnetic characterization of bianisotropic metasurfaces on refractive substrates: General theoretical framework," *Ann. Phys.*, vol. 528, nos. 9–10, pp. 721–737, Oct. 2016.

[15] J. Kong, *Electromagnetic Wave Theory*. Hoboken, NJ, USA: Wiley, 1986.

[16] S. A. Tretyakov, D.-H. Kwon, M. Albooyeh, and F. Capolino, "Functional metasurfaces: Do we need normal polarizations?" in *Proc. 32nd Gen. Assembly Sci. Symp. Int. Union Radio Sci. (URSI GASS)*, Aug. 2017, pp. 1–3.

[17] M. Albooyeh, D.-H. Kwon, F. Capolino, and S. A. Tretyakov, "Equivalent realizations of reciprocal metasurfaces: Role of tangential and normal polarization," *Phys. Rev. B, Condens. Matter*, vol. 95, no. 11, p. 115435, Mar. 2017.

[18] K. Achouri and C. Caloz, "Controllable angular scattering with a bianisotropic metasurface," in *Proc. IEEE Int. Symp. Antennas Propag. USNC/URSI Nat. Radio Sci. Meeting*, San Diego, CA, USA, Jul. 2017, pp. 1489–1490.

[19] C. Menzel, C. Rockstuhl, and F. Lederer, "Advanced Jones calculus for the classification of periodic metamaterials," *Phys. Rev. A, Gen. Phys.*, vol. 82, p. 053811, Nov. 2010.

[20] M. M. Idemen, *Discontinuities in the Electromagnetic Field*. Hoboken, NJ, USA: Wiley, 2011.

[21] E. F. Kuester, M. A. Mohamed, M. Piket-May, and C. L. Holloway, "Averaged transition conditions for electromagnetic fields at a metafilm," *IEEE Trans. Antennas Propag.*, vol. 51, no. 10, pp. 2641–2651, Oct. 2003.

[22] C. Pfeiffer and A. Grbic, "Emulating nonreciprocity with spatially dispersive metasurfaces excited at oblique incidence," *Phys. Rev. Lett.*, vol. 117, Aug. 2016, Art. no. 077401.

[23] G. Lavigne, K. Achouri, V. S. Asadchy, S. A. Tretyakov, and C. Caloz, "Susceptibility derivation and experimental demonstration of refracting metasurfaces without spurious diffraction," *IEEE Trans. Antennas Propag.*, vol. 66, no. 3, pp. 1321–1330, Mar. 2018.

[24] J. F. Cornwell, *Group Theory in Physics: An Introduction*, vol. 1. New York, NY, USA: Academic, 1997.

Authorized licensed use limited to: EPFL LAUSANNE. Downloaded on July 07,2020 at 09:05:10 UTC from IEEE Xplore. Restrictions apply.

Karim Achouri received the B.Sc. degree in microengineering and the M.Sc. degree in photonics and applied optics as well as a minor in space technologies from the Swiss Federal Institute of Technology in Lausanne (EPFL), Lausanne, Switzerland, in 2010 and 2012, respectively, and the Ph.D. degree in electromagnetics from the Polygrames Research Center, Ecole Polytechnique de Montréal, Montreal, QC, Canada, in 2017.

In 2013, he joined the Polygrames Research Center, Ecole Polytechnique de Montréal. In 2017, he joined the Nanophotonics and Metrology Laboratory (NAM), EPFL, as a Post-Doctoral Fellow. He is currently involved in the mathematical synthesis, the numerical analysis, and the practical realization of optical metasurfaces. His current research interests include electromagnetics, metamaterials, applied optics, photonics, and nanotechnologies.

Olivier J. F. Martin is currently a Professor of nanophotonics and optical signal processing with the Swiss Federal Institute of Technology, Lausanne (EPFL), Switzerland, where he is also the Head of the Nanophotonics and Metrology Laboratory and the Director of the Microengineering Section (approx. 800 students). He conducts a comprehensive research that combines the development of numerical techniques for the solution of Maxwell's equations with advanced nanofabrication and experiments on plasmonic systems. He has authored over 250 journal articles. He holds a handful of patents and invention disclosures. He received the ERC advanced grant on the utilization of plasmonic forces to fabricate nanostructures in 2016. His current research applications include metasurfaces, nonlinear optics, biosensing, heterogeneous catalysis, security features, and optical forces at the nanoscale.

Authorized licensed use limited to: EPFL LAUSANNE. Downloaded on July 07,2020 at 09:05:10 UTC from IEEE Xplore. Restrictions apply.